THE JOURNAL OF CELL BIOLOGY

Rapid pairing and resegregation of distant homologous loci enables double-strand break repair in bacteria

Anjana Badrinarayanan,[1] Tung B.K. Le,[1] and Michael T. Laub[1,2]

[1]Department of Biology and [2]Howard Hughes Medical Institute, Massachusetts Institute of Technology, Cambridge, MA 02139

Double-strand breaks (DSBs) can lead to the loss of genetic information and cell death. Although DSB repair via homologous recombination has been well characterized, the spatial organization of this process inside cells remains poorly understood, and the mechanisms used for chromosome resegregation after repair are unclear. In this paper, we introduced site-specific DSBs in *Caulobacter crescentus* and then used time-lapse microscopy to visualize the ensuing chromosome dynamics. Damaged loci rapidly mobilized after a DSB, pairing with their homologous partner to enable repair, before being resegregated to their original cellular locations, independent of DNA replication. Origin-proximal regions were resegregated by the ParABS system with the ParA structure needed for resegregation assembling dynamically in response to the DSB-induced movement of an origin-associated ParB away from one cell pole. Origin-distal regions were resegregated in a ParABS-independent manner and instead likely rely on a physical, spring-like force to segregate repaired loci. Collectively, our results provide a mechanistic basis for the resegregation of chromosomes after a DSB.

Downloaded from http://rupress.org/jcb/article-pdf/210/3/385/1591488/jcb_201505019.pdf by guest on 07 February 2026

Introduction

The maintenance of life requires the preservation of genomic integrity. Double-strand breaks (DSBs) are a particularly dangerous form of DNA damage and unrepaired or incorrectly repaired DSBs can result in genome rearrangements, loss of genetic information, mutations, or cell death (Symington and Gautier, 2011; Lenhart et al., 2012). Cells from all three domains of life can faithfully repair a DSB via homologous recombination, using an unbroken, homologous copy of DNA as a template to repair the lesion. Thus, a broken region must be able to search for, and find, its homologous partner within the cell (Alonso et al., 2013; Wigley, 2013). The spatial dynamics of homology searching and DSB repair, which could involve the movement of chromosomal regions over long distances, remain poorly understood in all organisms.

The biochemical events underlying homologous recombination have been studied extensively, particularly in *Escherichia coli* (Dillingham and Kowalczykowski, 2008). One strand of each broken chromosomal end is resected by the helicase–nuclease complex RecBCD (Wigley, 2013; Krajewski et al., 2014). The single-stranded DNA (ssDNA) binding protein RecA is then recruited to the break site where it forms a filament along the DNA. This RecA-based nucleoprotein structure, and other repair proteins, then drives homologue pairing and subsequent repair of the DSB (Dillingham and Kowalczykowski, 2008; Lesterlin et al., 2014). Although the steps of homologous recombination-based DNA repair have been thoroughly dissected, less is known about the spatial aspects of sister chromosome pairing and the subsequent resegregation of repaired regions in vivo.

The Gram-negative bacterium *Caulobacter crescentus* is an excellent system for investigating chromosome dynamics during DSB repair as cells can be easily synchronized with respect to the cell cycle and because the chromosome is organized in a stereotypical manner throughout a population of cells (Fig. 1 A). DNA replication in *C. crescentus* occurs only once per cell division, with each daughter cell inheriting a single, fully replicated chromosome. Microscopy and Hi-C studies have demonstrated that each chromosome produced after DNA replication is tethered to a cell pole by an origin-proximal locus with the two chromosome arms running in parallel down the long axis of the cell and the terminus near mid-cell; individual loci are positioned, relative to the polar origin, in the same approximate order that they appear in the genome sequence (Viollier et al., 2004; Le et al., 2013).

This pattern of chromosome organization is established primarily by the segregation of newly replicated origins to opposite cell poles via the ParA-ParB-*parS* system (Mohl et al., 2001; Toro et al., 2008; Lim et al., 2014; summarized in Fig. 1 A). DNA replication initiation results in the duplication

Correspondence to Michael T. Laub: laub@mit.edu

Abbreviations used in this paper: DSB, double-strand break; MMC, mitomycin C; ssDNA, single-stranded DNA.

© 2015 Badrinarayanan et al. This article is distributed under the terms of an Attribution–Noncommercial–Share Alike–No Mirror Sites license for the first six months after the publication date (see http://www.rupress.org/terms). After six months it is available under a Creative Commons License (Attribution–Noncommercial–Share Alike 3.0 Unported license, as described at http://creativecommons.org/licenses/by-nc-sa/3.0/).

The Rockefeller University Press $30.00
J. Cell Biol. Vol. 210 No. 3 385–400
www.jcb.org/cgi/doi/10.1083/jcb.201505019

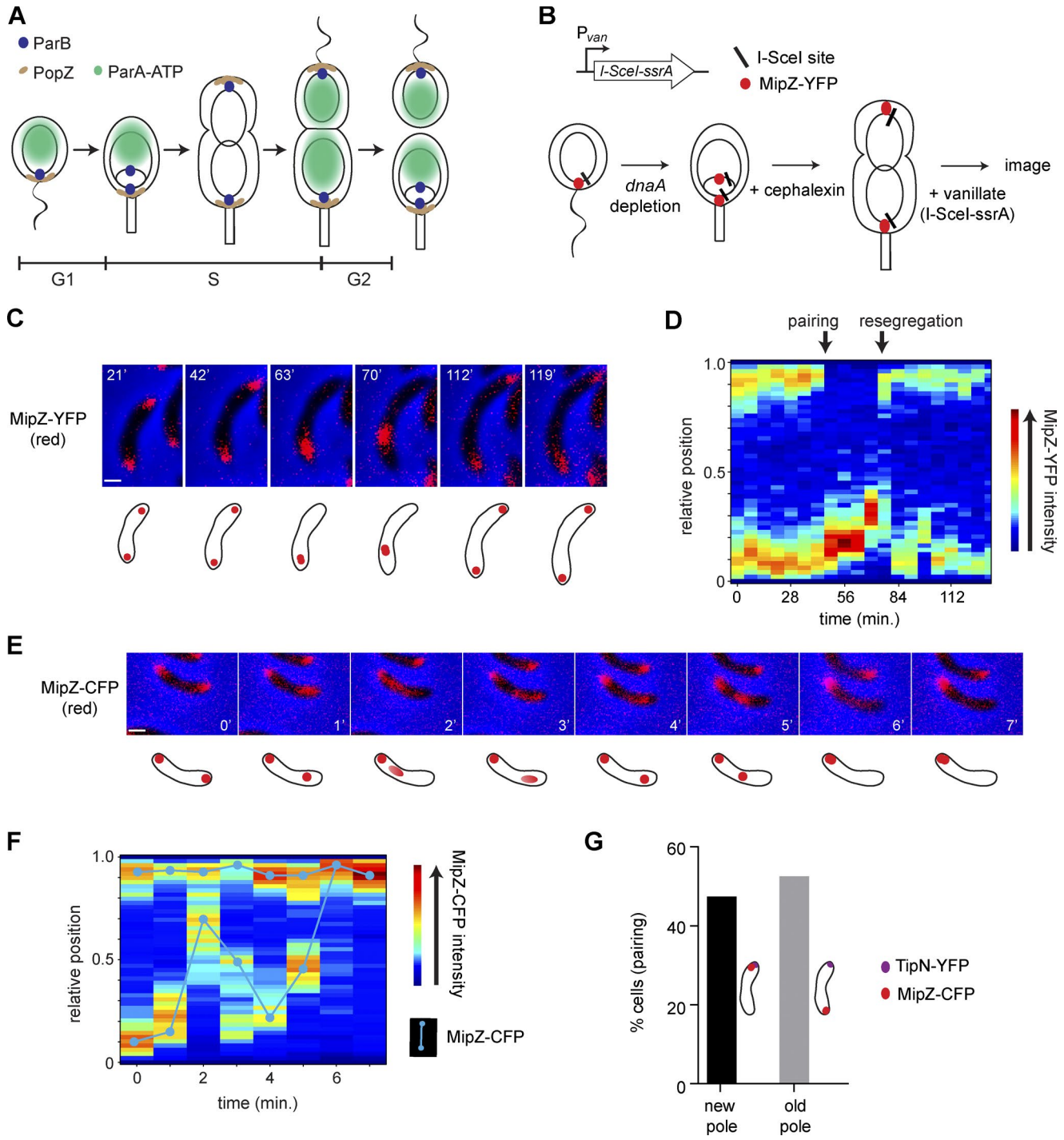

Figure 1. **Monitoring chromosome dynamics after a site-specific DSB in *C. crescentus*.** (A) Schematic of the *C. crescentus* cell cycle. Proteins involved in origin segregation are highlighted. (B) Summary of the system used to introduce a site-specific DSB 30 kb from the origin of replication. I-SceI enzyme is under the control of a vanillate-inducible promoter on the chromosome. Nonreplicating predivisional cells were isolated by synchronization followed by depletion of DnaA (leading to exactly two chromosomes) and addition of cephalexin (to block cell division). Dynamics of the origin region were visualized with MipZ-YFP. Vanillate was added at the start of the time-lapse imaging to induce I-SceI. (C) Representative time-lapse imaging of MipZ-YFP pairing and resegregation in predivisional cells during DSB repair. Schematic of the cell imaged is shown below. (D) Kymograph of MipZ-YFP signal from cell in C shows pairing of MipZ foci, producing an increase in focus intensity, and subsequent resegregation of the paired foci to opposite cell poles. Images were taken every 7 min. (E) Time-lapse microscopy showing pairing dynamics after a DSB occurring 30 kb from the origin. Images taken every 1 min. (F) Kymograph of MipZ-YFP signal from cell in E. (G) Pairing of MipZ-CFP during DSB repair is independent of the cell pole. The new cell pole was marked using TipN-YFP, and origin dynamics were followed with MipZ-CFP. Percentage of cells with MipZ pairing at old or new pole are shown, $n = 75$ from a representative experiment out of three independent repeats. Bars, 1 µm.

Downloaded from http://rupress.org/jcb/article-pdf/210/3/385/1591488/jcb_201505019.pdf by guest on 07 February 2026

of the origin-proximal *parS* site bound by ParB. Although one *parS*–ParB complex remains associated with the old cell pole, the second *parS*–ParB complex is thought to contact a cloud of ATP-bound ParA bound nonspecifically to DNA that emanates from the opposite cell pole. ParB stimulates an intrinsic ATPase activity of ParA, releasing it from the DNA. The net result is a retraction of the ParA-ATP cloud and subsequent movement of the *parS*–ParB complex toward the opposite cell pole (Ptacin et al., 2010; Schofield et al., 2010). This process repeats until one ParB–*parS* complex moves across the cell where it becomes anchored to the cell pole by the polarly localized protein PopZ. (Bowman et al., 2008; Ebersbach et al., 2008).

How the rest of the chromosome is segregated after one origin translocates to the opposite cell pole remains unclear (Wang et al., 2013). The polarly anchored origins may help orient bulk chromosome segregation with DNA extruded from replication forks moving to opposite sides of the cell. Whatever the mechanism, loci distal to the origins are probably not actively translocated by a dedicated system akin to ParABS.

Importantly, once duplicated loci are segregated to opposite sides of the predivisional *C. crescentus* cell, they remain relatively stationary until the next round of replication, and the ParA cloud that drives origin translocation disperses after the origins are positioned at opposite poles. Thus, it remains unclear whether, and how, chromosomal loci, either proximal to or distal from the origin, move to enable homologous recombination should a DSB occur. In *E. coli*, distant loci can move and pair after a DSB in a RecA-dependent manner, but whether pairing occurs independently of DNA replication has not been established (Lesterlin et al., 2014). Additionally, unlike *C. crescentus* and nearly 65% of all other bacteria (Livny et al., 2007), *E. coli* does not encode a ParABS system, so the role of this partitioning system in chromosome mobility during DNA repair is unknown.

Here, we used an inducible restriction enzyme, I-SceI (Monteilhet et al., 1990), to introduce DSBs in *C. crescentus* and then study chromosome dynamics during and after DNA repair. We find that DSB repair occurs without ongoing DNA replication and that even distant, fully segregated regions of the chromosome, including the polarly tethered origin-proximal regions, can pair and resegregate after a DSB. We find that a region of ~130 kb on either side of a DSB moves during the homology search, with little impact on global chromosome organization. Resegregation of a repaired, origin-proximal region requires the ParABS system, with formation of the ParA structure involved occurring dynamically in response to the displacement of an origin from the cell pole. This pattern suggests that the movement of origin-associated ParB, which normally promotes ATP hydrolysis by ParA, enables pole-proximal accumulation of ParA-ATP, which can then promote the rapid resegregation of the origin after DNA repair is completed. In contrast, the resegregation of origin-distal loci that moved to repair a DSB, occurs without using the ParABS system, and likely relies on a physical mechanism and the relaxation of chromosomal DNA back to its initial cellular position after repair.

Results

Monitoring chromosome dynamics after a site-specific DSB

To study chromosome dynamics after a DSB in *C. crescentus*, we engineered a system for site-specifically introducing a DSB on the chromosome (Fig. 1 B). A single I-SceI recognition site (Monteilhet et al., 1990), not present in the wild-type *C. crescentus* genome, was introduced +30 kb from the origin of replication, and the I-SceI endonuclease, which produces a DSB upon cleavage, was expressed from a vanillate-inducible promoter, P_{van}, on the chromosome. To ensure that I-SceI was produced at sufficiently low levels that most cells experience only a single DSB, we added a C-terminal *ssrA* tag to destabilize I-SceI. Induction of I-SceI-*ssrA* reduced cell viability with increasing concentrations of vanillate (Fig. S1 A). To confirm that induction of I-SceI produces a site-specific DSB, we performed semiquantitative PCR with primers flanking the cut site. After inducing I-SceI-*ssrA* for 1 h, we observed a 6.4-fold decrease in PCR product compared with a control region on the chromosome (Fig. S1 B).

To control the state of DNA replication during induction of DSBs, we placed the gene encoding the replication initiator DnaA under control of an IPTG-inducible promoter, P_{lac}. Cell populations were synchronized by isolating G1 swarmer cells and then shifting to a growth medium without IPTG to deplete DnaA; cells have enough DnaA to initiate one round of DNA replication but then cannot reinitiate (Chen et al., 2011). We also added the antibiotic cephalexin to block cell division. At 80 min after synchronization, cells had reached the predivisional stage, and harbored two fully replicated and segregated chromosomes, but without an intervening septum. Subcellular localization and temporal dynamics of the origin region were tracked by visualizing MipZ-YFP with time-lapse fluorescence microscopy; MipZ interacts directly with ParB bound to *parS* sites near the origin (Thanbichler and Shapiro, 2006; Kiekebusch et al., 2012), ~38 kb from the DSB site (Fig. 1 B).

Segregated chromosomal regions can pair independent of DNA replication

Using our system for monitoring chromosome dynamics, we found that when no DSB was induced (no vanillate added), cells had two MipZ-YFP foci localized to opposite cell poles throughout a time-lapse experiment, as expected (Fig. S1, C and D). When vanillate was added to induce DSBs, most (62%) cells exhibited a loss of MipZ-YFP localization from one cell pole with a concomitant increase in the fluorescent signal from the focus at the opposite cell pole (Fig. 1, C and D). These events likely reflect the introduction of a DSB in one of the two chromosomes, with a region around the break having translocated across the cell to pair with its sister chromosome, enabling DNA repair by homologous recombination. We conclude that it is the damaged chromosome that moves to pair with its undamaged sister, not vice versa, because inducing DSBs in cells harboring a single chromosome also increased locus mobility substantially (unpublished data).

The initial pairing of loci after a DSB typically occurred within a single 7-min frame of time-lapse imaging. To better visualize pairing dynamics, we also imaged cells at 1-min intervals. Although pairing still often occurred within a single frame of imaging, we could observe dynamic movement of a MipZ focus before pairing in ~20% of cells. For such cells, the movement of individual MipZ foci was not unidirectional (in the x–y plane imaged), moving initially toward the other MipZ focus, but sometimes reversing direction along the long axis of the cell (Fig. 1, E and F; and Fig. 2 A), suggesting that the damaged chromosome engages in a homologue search, not directional movement. Eventually, the mobile focus merged with the more

Downloaded from http://rupress.org/jcb/article-pdf/210/3/385/1591488/jcb_201505019.pdf by guest on 07 February 2026

static MipZ focus, forming a single focus that likely represents a successful pairing of homologous loci.

Homologous pairing events were not biased to occur at either the new (swarmer) or old (stalked) cell pole. Using TipN-YFP as a marker of the new cell pole (Huitema et al., 2006; Lam et al., 2006), we found that pairing occurred with similar frequencies at the two poles (Fig. 1 G). This result is consistent with the notion that whichever chromosomal region suffers a DSB translocates across the cell to pair with its undamaged, homologous partner to promote repair.

In our conditions (cells imaged for 2.3 h on agarose pads supplemented with 2 μM vanillate), pairing occurred in 62 ± 2% of cells, whereas 16 ± 2% of cells retained two polarly localized MipZ foci throughout the experiment (Fig. 2 B), likely because they did not experience a DSB. In 22 ± 4% of cells, both MipZ foci disappeared, presumably because a DSB occurred on both chromosomes, preventing repair by homologous recombination, with exonuclease activity eventually eliminating both *parS* sites and, consequently, the two MipZ foci (Fig. 2 B).

Finally, to test whether DnaA depletion or cephalexin addition affects the DSB-induced chromosome dynamics and homologue pairing observed, we also induced DSBs using the I-SceI system but in an asynchronous population of cells. We observed the pairing of MipZ foci in a similar percentage of cells as before (Fig. S2 A).

Paired chromosomal regions resegregate to their original locations after repair

Of the cells in which pairing occurred, approximately half resolved with resegregation of origin foci to opposite poles, whereas the other half remained paired for the duration of the imaging (Fig. 2 B). Cells that retained a single focus had often exhibited delayed pairing initially and thus might not have been imaged long enough to observe resegregation, or such cells experienced a second DSB before resegregation occurred. For those foci that resolved, pairing lasted 32 ± 9 min before resegregation to opposite cell poles occurred, setting an approximate upper bound on the time needed to repair a lesion.

Unlike the initial pairing process (Fig. 2 A), the resegregation of MipZ-CFP foci exhibited very few reversals on the long axis of cells, similar to that observed during the segregation of newly replicated origins in wild-type cells (Fig. 2 C). Time-lapse imaging with 1- or 2-min sampling indicated that one MipZ focus typically remained at the pole where pairing occurred, whereas the other focus moved toward the other pole at a more constant rate compared with the initial pairing process. Although we did not observe large reversals in focus movement along the long axis of the cell, we cannot rule out reversals occurring on a time scale faster than our sampling or on shorter spatial scales than can be resolved by epifluorescence microscopy.

In cells in which pairing occurred and was subsequently resolved, the paired MipZ foci typically remained polarly localized until one focus was segregated to the opposite pole. However, in ∼15% of cells, the paired MipZ foci drifted away from the pole where pairing initially occurred. In such cases, resegregation involved the movement of one focus to the nearest pole with the other focus translocating across the cell to the opposite pole (Fig. S2, B, C, G, and H).

To confirm that the dynamics of MipZ during pairing and resegregation were faithfully reflecting the dynamics of the origin-proximal region of chromosomes, we simultaneously visualized CFP-ParB and MipZ-YFP in cells experiencing DSBs. Similar pairing and resegregation dynamics were observed for ParB and MipZ foci, and they remained colocalized throughout a typical time-lapse experiment (Fig. S2 D).

Altogether, our results thus far indicate that homology searching and DSB repair can occur independently of DNA replication. Initially distant and segregated regions of the chromosome can move and rapidly pair with a sister chromosome after a DSB, before being resegregated after repair. Although chromosomal loci in bacteria are often portrayed as relatively stably positioned after DNA replication, our results indicate that they retain the potential for significant long-range mobility, beyond subdiffusive motion.

RecA is required for long-range movement of damaged loci but does not initiate an SOS response

The aforementioned chromosomal dynamics were strongly dependent on factors required for homologous recombination-based repair. Cells subjected to an I-SceI–induced DSB, but lacking AddAB, the helicase and nuclease that process DSBs to reveal ssDNA (Wigley, 2013), or lacking RecA, which binds ssDNA and ultimately promotes strand exchange (Cromie et al., 2001), did not successfully repair, as *addAB* and *recA* cells did not exhibit focus pairing or resegregation (Fig. S2 E). For cells lacking RecN, which is thought to hold DSB ends together (Pellegrino et al., 2012), ∼4% of cells exhibited dynamics consistent with DNA repair.

To further probe the role of RecA in the chromosome dynamics underlying DSB repair, we sought to visualize RecA-YFP. We were unable to replace RecA with a fully functional tagged version at its endogenous locus. We therefore constructed a strain producing RecA-YFP at low levels from a xylose-inducible promoter, P_{xyl}, in the presence of wild-type RecA. In these cells, the induction of a DSB led to the formation of either a RecA-YFP focus or an extended, elongated structure (Fig. 2, D and E); we refer to these latter structures as filaments, although we cannot say yet whether they are continuous polymers of RecA. Time-lapse imaging indicated that, in 50 ± 4% cells, these RecA-YFP filaments localized initially near the MipZ-CFP focus that eventually translocated across the cell (Fig. 2 E and Fig. S2 F). RecA-YFP filaments dispersed during or after the pairing process, sometimes briefly forming a focus away from the paired MipZ foci. Once resegregation began, RecA-YFP fluorescence was typically distributed homogenously across the cell, as it was before DSB induction. These dynamics are reminiscent of those seen in *E. coli* (Lesterlin et al., 2014) and suggest that RecA helps drive or promote the homologue search process.

RecA filaments that form on ssDNA represent the primary signal for SOS induction by promoting cleavage of the transcription repressor LexA (Erill et al., 2007). To test whether the SOS response is activated in *C. crescentus* cells after a DSB, we used a reporter in which YFP is driven by the LexA-regulated promoter of *sidA* (Modell et al., 2011). A low-copy plasmid carrying P_{sidA}-*yfp* was transformed into a strain harboring the I-SceI system, predivisional cells were isolated, and DSBs were induced by adding vanillate for 1 h. As a positive control, predivisional cells were separately treated with 1 μg/ml mitomycin C (MMC; Modell et al., 2011). We measured the fold increase in YFP intensity of damage-induced cells relative to untreated predivisional cells (Fig. 2 F). MMC induced a 4.4-fold increase in YFP signal, on average. In contrast, I-SceI–induced DSBs

Downloaded from http://rupress.org/jcb/article-pdf/210/3/385/1591488/jcb_201505019.pdf by guest on 07 February 2026

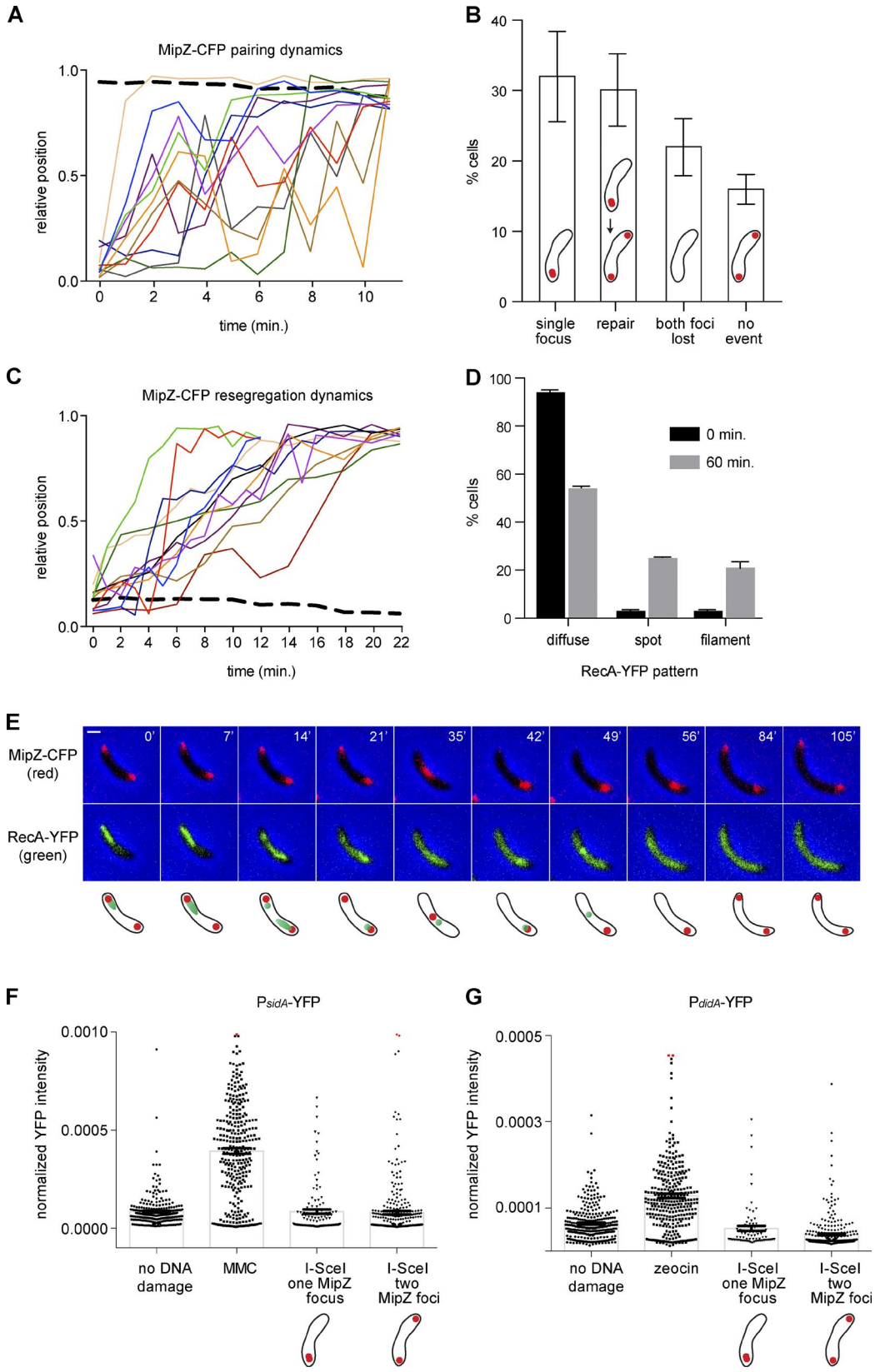

Figure 2. **Paired chromosomal regions resegregate to their original locations after repair.** (A) MipZ-CFP pairing dynamics. Each trace represents the position and movement of a MipZ focus during pairing in an individual cell. Black dotted line represents the mean position of the second MipZ focus. Images were taken every 1 min. (B) Summary of MipZ dynamics after 2.3 h of imaging for cells that each started with two MipZ foci. Error bars represent SD, n = 200 from three independent repeats. (C) MipZ-CFP resegregation dynamics. Each trace represents the position and movement of a MipZ focus during resegregation in an individual cell. Black dotted line represents the mean position of the second MipZ focus during resegregation. (D) Summary of RecA-YFP localization patterns 0 and 60 min after DSB induction. Error bars represent SD, n = 200 cells in each case from two independent repeats. (E) Time-lapse

Downloaded from http://rupress.org/jcb/article-pdf/210/3/385/1591488/jcb_201505019.pdf by guest on 07 February 2026

did not produce a strong *sidA* induction in cells where MipZ pairing had occurred. We conclude that although a single DSB does not induce the SOS response, it does induce the formation of RecA foci and filaments.

C. crescentus also has an SOS-independent, but still DNA damage-induced, response mediated by the transcription factor DriD (Modell et al., 2014). To test whether this pathway was activated by a single DSB, we also assessed the induction of a YFP reporter driven by the *didA* promoter (Modell et al., 2014). As a positive control, predivisional cells were separately treated with 15 µg/ml zeocin, which is known to induce a DriD-dependent response (Modell et al., 2014). Although treatment with zeocin resulted in an approximate twofold increase in YFP intensity, we did not observe a significant increase in YFP intensity in cells treated with I-SceI (Fig. 2 G). Collectively, our findings suggest that cells can cope with a single DSB without inducing a transcriptional program and therefore use baseline levels of DSB repair proteins.

Homologue pairing involves ~250–300 kb flanking a DSB but does not affect global chromosome organization

The aforementioned results involved the introduction of a DSB ~38 kb from the chromosomal region, *parS*, being imaged via fluorescently tagged MipZ or ParB. To assess how much of the chromosome translocates in cells that experience a DSB, we used an orthogonal *parS*–ParB system from plasmid pMT1 (Nielsen et al., 2006; Le and Laub, 2014) to visualize loci at varying distances from the I-SceI cut site that was ~30 kb from the origin. $parS^{pMT1}$ sites introduced 20, 70, −2, −80, or −130 kb from the I-SceI cut site were visualized by expressing YFP-tagged $ParB^{pMT1}$, whereas the native *parS* site was visualized by monitoring CFP-tagged MipZ. $parS^{pMT1}$ sites introduced 170, 770, −230, or −830 kb from the I-SceI cut site were visualized with CFP-tagged $ParB^{pMT1}$ and the native *parS* site was visualized using YFP-tagged MipZ. Cells harboring two completely replicated and segregated chromosomes were isolated, with I-SceI induced 1 h before imaging. We then examined the subcellular localization of $ParB^{pMT1}$ in cells harboring a single focus of MipZ in which a DSB and subsequent homologue pairing had presumably occurred. For chromosomal regions within ~130 kb, on either side of the cut site, >70% of cells with one MipZ focus had one $ParB^{pMT1}$ focus (Fig. 3, A and B); for regions within ~40 kb, >95% of cells showed $ParB^{pMT1}$ and MipZ pairing. In contrast, for loci >170 kb from the cut site, most cells retained two $ParB^{pMT1}$ foci, indicating that these chromosomal regions were not mobilized during DSB repair.

Although only ~250–300 kb of chromosomal DNA moves, a DSB could still impact chromosome compaction or organization more globally. To assess the possible effects of a DSB on global chromosome organization, we used chromosome conformation capture with deep sequencing, or Hi-C (Le et al., 2013). Prior Hi-C analysis of undamaged cells demonstrated that the *C. crescentus* chromosome contains ~23 chromosomal interaction domains where loci interact preferentially with other loci in the same domain. Here, we performed Hi-C on cells experiencing a DSB near the origin of replication (Fig. 3 C). We used I-SceI to induce DSBs in nonreplicating swarmer cells harboring only a single chromosome, which facilitates Hi-C analysis. The Hi-C map generated was highly similar to undamaged swarmer cells (r = 0.9). In each case, the highest scores occurred along the main diagonal, reflecting short-range interactions between loci on the same chromosomal arm, with lower scores on the opposite diagonal, resulting from inter-arm interactions. The chromosomal interaction domains in each case were of similar size and at similar locations. This comparison suggests that global chromosome organization is maintained after a DSB, despite the induced movement of ~250–300 kb of DNA. The maintenance of global chromosome organization may contribute to an efficient homology search and to the resegregation of loci after repair.

To test whether the amount of DNA that moves after a DSB depends on the location of the cut site, we created strains in which an I-SceI site was introduced ~121 or ~216 kb from the origin of replication. We then visualized the cut site using YFP-$ParB^{pMT1}$ and a $parS^{pMT1}$ site inserted ~11 or 16 kb, respectively, from the I-SceI site, while simultaneously monitoring the origin region using MipZ-CFP. For a DSB occurring ~121 kb from the origin, YFP-$ParB^{pMT1}$ and MipZ-CFP both paired and formed a single focus in 60 ± 6% of cells (Fig. 4 A). During resegregation, MipZ-CFP movement preceded YFP-$ParB^{pMT1}$. For a DSB ~216 kb from the origin, the *parS*-YFP-$ParB^{pMT1}$ reporter near the cut site again showed pairing and resegregation, but usually independent of MipZ and the origin, with MipZ-CFP movement observed in only 12 ± 3% of cells (Fig. 4 B). As with the origin region (Fig. 2 C), resegregation of the 110- and 200-kb markers after DSB pairing was predominantly a directional process with no major reversals along the long axis of the cell (Fig. 4, C and D). In sum, our results indicate that ~130–150 kb on either side of a DSB, translocates during homologue pairing regardless of where the DSB occurs.

ParA is essential for segregation of the origin region after DSB repair

Because only a limited region of DNA moved after a DSB, we wondered whether the resegregation of repaired loci was passive or active, and if active, whether it depended on ParABS, which help segregate undamaged, newly replicated chromosomes. To assess the role of ParA in segregating loci after DSB repair in nonreplicating cells, we first examined ParA-YFP in cells carrying an I-SceI site near the origin of replication and producing MipZ-CFP to label the origins (Fig. 5, A and B). Upon DSB induction, the pairing of MipZ-CFP foci was accompanied by the formation of a cloud of ParA-YFP with maximum intensity near the cell pole opposite the paired MipZ foci. The change in ParA-YFP localization occurred at approximately the same time as MipZ-CFP focus pairing. During resegregation, the ParA-YFP structure appeared to retract toward the pole, coincident with the MipZ foci moving to opposite poles. Once MipZ foci were localized back at opposite cell poles,

microscopy of a cell producing RecA-YFP and MipZ-CFP and subjected to a DSB. Schematics summarizing the patterns observed are shown below. Bar, 1 µm. (F and G) A single DSB does not induce a DNA damage transcriptional response. Induction of P_{sidA} (F) or P_{didA}-YFP (G) was assessed in predivisional cells after DSB induction for 1 h. As positive controls, cells carrying the P_{sidA} or P_{didA} reporter were treated with 1 µg/ml MMC or 15 µg/ml zeocin, respectively, for 1 h. YFP intensity was normalized to cell area. Bars indicate the mean, and error bars represent SEM. Symbols indicate YFP intensity for individual cells. Red symbols represent values outside the range of the graph. $n \geq 120$ in each case from a representative experiment out of two independent repeats.

Downloaded from http://rupress.org/jcb/article-pdf/210/3/385/1591488/jcb_201505019.pdf by guest on 07 February 2026

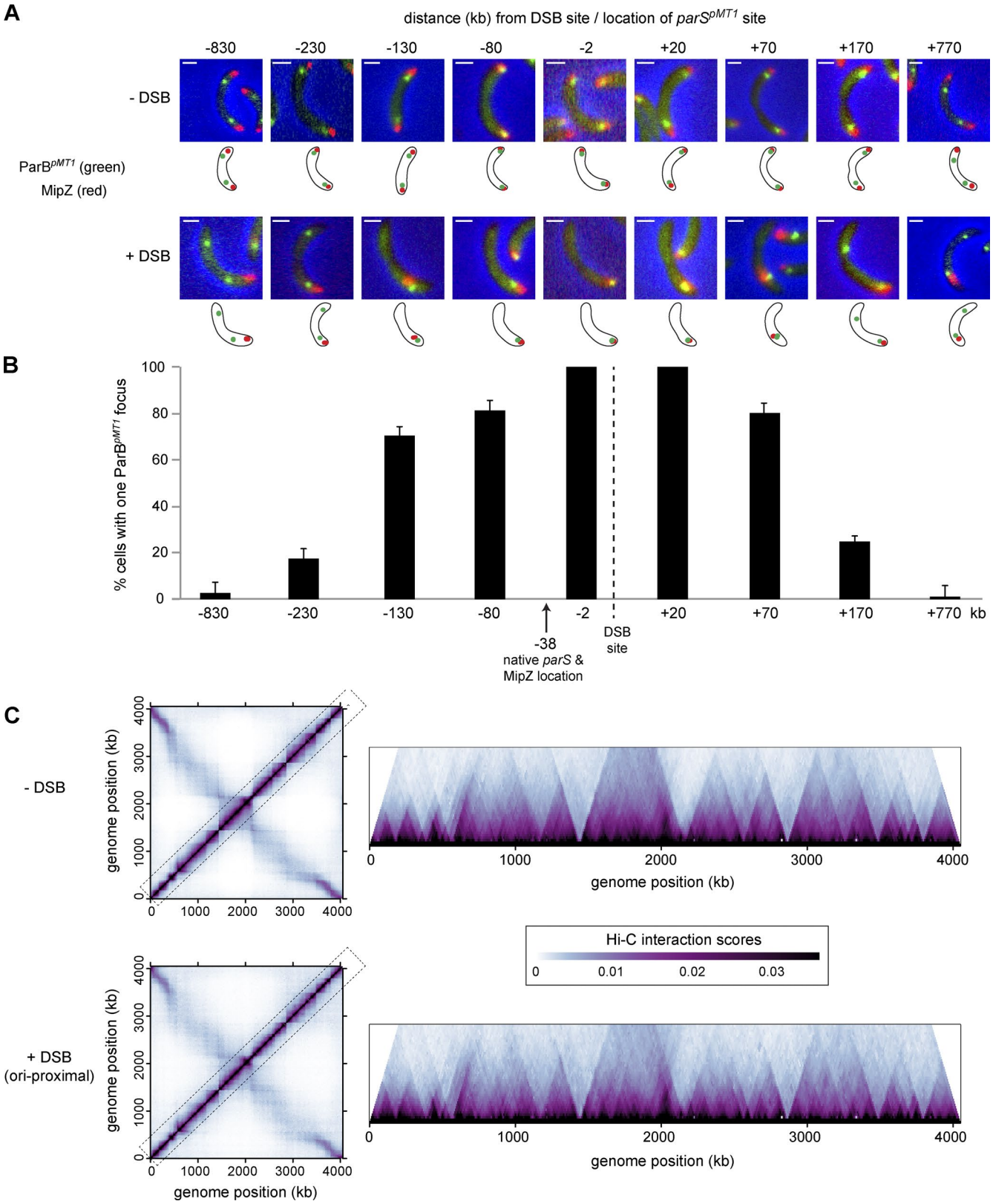

Figure 3. **Homologue pairing involves ~250–300 kb flanking a DSB, but does not affect global chromosome organization.** (A) An orthogonal *parS*–ParB system from plasmid pMT1 was used to visualize loci at various locations on the chromosome indicated by their distance from the I-SceI site where a DSB occurs, which was at a site 30 kb from the origin. Representative cells before (above) and 1 h after (below) I-SceI induction are shown. Bars, 1 μm. (B) Percentage of cells with one ParB^{pMT1} focus (marking the chromosomal locations indicated, as in A); only cells with one paired MipZ focus, indicating occurrence of a DSB, were considered. The location of the native *parS*, which MipZ associates with via ParB, and the DSB site are indicated. Error bars represent SD. $n \geq 100$ cells from at least two independent repeats. (C) Hi-C maps of nonreplicating swarmer cells without or with a DSB indicate that chromosomal interaction domains are maintained. The I-SceI site was 30 kb from the origin of replication. Hi-C scores are color coded according to the legend shown. ori, origin.

Downloaded from http://rupress.org/jcb/article-pdf/210/3/385/1591488/jcb_201505019.pdf by guest on 07 February 2026

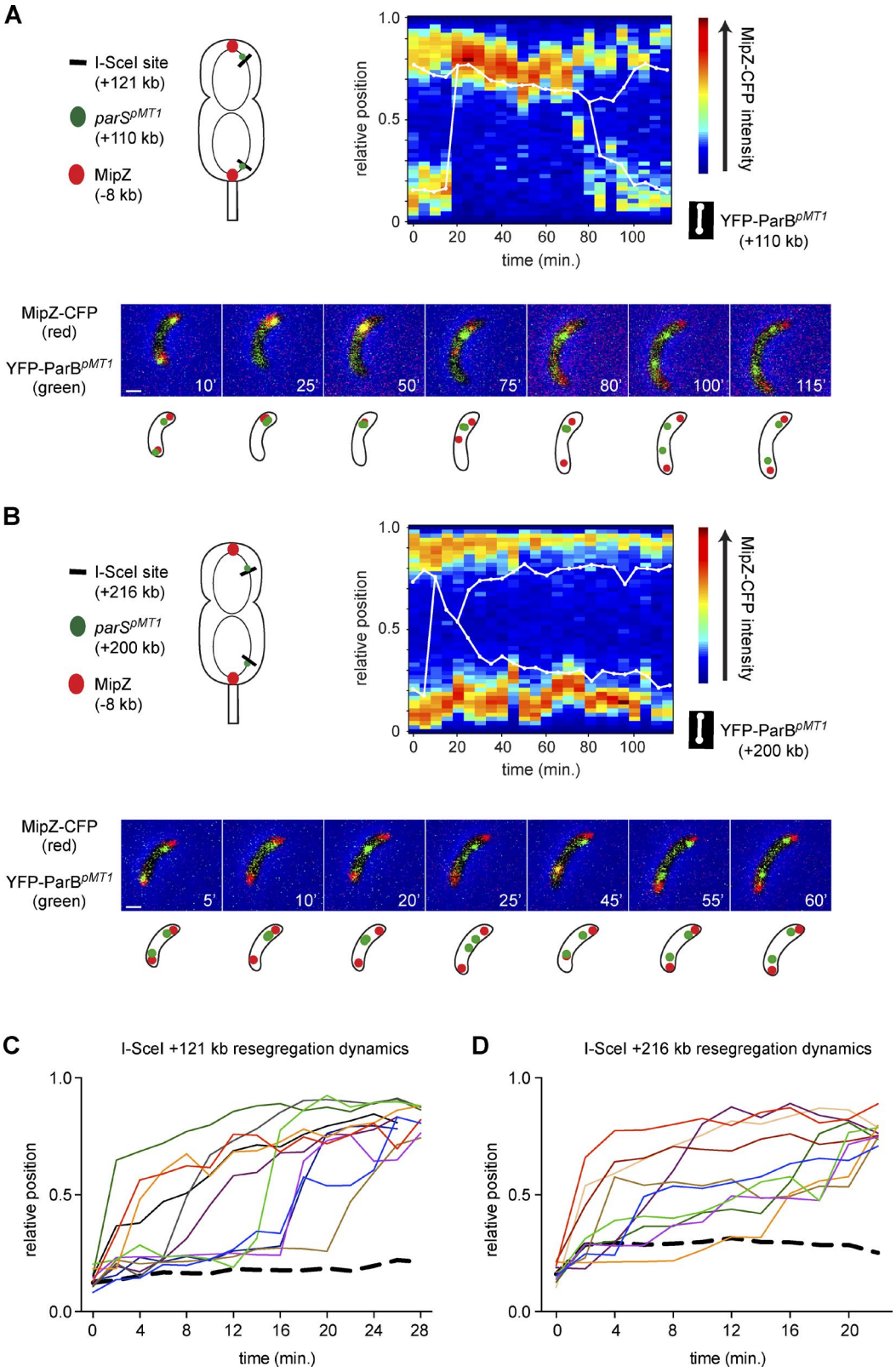

Figure 4. **Pairing of an origin-proximal region only occurs after an origin-proximal DSB.** (A) An I-SceI site was inserted 121 kb from the origin. Dynamics of the cut-site were visualized via a *parS*^{pMT1} site inserted ~11 kb from the cut site and YFP-ParB^{pMT1}; dynamics of the origin were followed by tracking MipZ-CFP. Kymograph shows MipZ-CFP dynamics with a trace (white line) indicating YFP-ParB^{pMT1} dynamics after a DSB. Images were taken every 5 min. A subset of images is shown below with schematics summarizing the localization of MipZ-CFP and YFP-ParB^{pMT1}. (B) As in A, but with the I-SceI site inserted 216 kb from the origin and *parS*^{pMT1} inserted ~16 kb from the cut site. (C) YFP-ParB^{pMT1} resegregation dynamics when a DSB is induced 121 kb from the origin with a *parS*^{pMT1} site 110 kb from the origin. Each trace represents an individual cell. Black dotted line represents the mean position of the second YFP-ParB^{pMT1} focus during the resegregation process. (D) YFP-ParB^{pMT1} resegregation dynamics when a DSB is induced 216 kb from the origin and a *parS*^{pMT1} site is 200 kb from the origin. Bars, 1 µm.

Downloaded from http://rupress.org/jcb/article-pdf/210/3/385/1591488/jcb_201505019.pdf by guest on 07 February 2026

ParA-YFP fluorescence was again distributed relatively uniformly across the cell. In cells where the paired MipZ foci drifted away from the pole before segregation, ParA-YFP clouds formed on both sides of the MipZ-CFP foci and each retracted until the MipZ foci relocalized to opposite poles (Fig. S2, G and H). The time taken from MipZ focus pairing to resegregation correlated strongly with the time interval between ParA cloud formation and dispersal (Fig. 5 C), supporting the notion that ParA promotes resegregation of repaired, origin-proximal loci. Collectively, our results indicate that ParA clouds can form at either pole, or sometimes both poles; in contrast, during the segregation of undamaged chromosomes the ParA cloud forms only at the new, swarmer pole.

To test whether ParA was necessary to resegregate origin-proximal regions of the chromosome after DSB repair occurs, we introduced an inducible copy of the dominant-negative mutant *parA(K20R)* (Toro et al., 2008) at the P_{xyl} locus. The ParA(K20R) mutant was induced for 60 min before imaging cells experiencing a DSB. MipZ-CFP focus pairing occurred in a similar percentage of cells as before, but now no cells completely resegregated the MipZ foci to opposite poles, and only 15% of cells showed partial MipZ resegregation or focus separation (Fig. 5, D–F). In contrast, for cells producing only wild-type ParA, ~52% of paired MipZ foci resegregated. These results indicate that ParA activity is essential for resegregating the origin-proximal region after repair of a nearby DSB.

Notably, in cells expressing ParA(K20R), most MipZ foci did not resegregate, nor did they even separate enough to produce two separate foci. In contrast, in undamaged, wild-type cells, ParA(K20R) prevents the full segregation of newly replicated origins to opposite cell poles, but the origin regions still separate and two distinct foci can be resolved (Toro et al., 2008; Shebelut et al., 2010). Thus, we suggest that the initial separation of newly replicated origins may depend on DNA replication, with the physical act of replication and bulk chromosome accumulation potentially providing the force, and ParA then driving complete segregation. In the cells examined here, where DSBs are induced after replication has been completed, the MipZ foci remain paired.

PopZ is required for robust origin resegregation after DSB repair

The origin-proximal region of the chromosome is anchored to the cell pole via an interaction of the *parS*–ParB complex with PopZ, and PopZ has been suggested to directly modulate ParA activity during origin segregation in replicating cells (Ptacin et al., 2014). To probe the role of PopZ in chromosome segregation after DSB repair, we first examined whether PopZ localization changes after a DSB. We found that PopZ-YFP remained bipolarly localized throughout the process of DSB repair (Fig. S3, A and B). In a minority of cells, we observed a third, weak PopZ-YFP focus near mid-cell, which may form in the DNA-free region between segregated *ter* regions of the two replicated chromosomes.

Next, we examined the DSB repair process in cells lacking *popZ*. DSB induction in Δ*popZ* cells still resulted in the pairing and subsequent resegregation of MipZ-CFP foci (Fig. S3, C–F). However, MipZ foci were not as stationary after pairing (Fig. S3, C and D), and resegregation was no longer a robust and apparently directional process (Fig. S3, C–E, red arrows). Interestingly, in Δ*popZ* cells that have multiple MipZ foci (resulting from the cell division defect of Δ*popZ* cells), we observed the pairing and resegregation of MipZ foci initially located quite distant from the cell poles (Fig. S3 F).

To better probe the role of PopZ in chromosome segregation after DSB repair, we constructed a system for inducing the degradation of PopZ, replacing the wild-type *popZ* with *popZ-YFP-pcDAS4*, which can be specifically degraded by inducing *E. coli* SspB from a xylose-inducible promoter (Rood et al., 2012). Induction of *E. coli sspB* for 6 h reduced the levels of PopZ-YFP by ~70% (Fig. S3, G–I). We then induced the degradation of PopZ-YFP-pcDAS4 in a mixed population of cells for 4.5 h, harvested swarmer cells, and grew them for 1.5 h as before, blocking DNA replication and cell division while inducing a DSB. The induction of a DSB resulted in the pairing of MipZ-CFP foci. However, as with Δ*popZ* cells, MipZ resegregation was no longer as robust, with foci often exhibiting several back-and-forth movements before reaching opposite cell poles (Fig. S3 I). Additionally, before their separation, paired foci flipped to the opposite pole in ~50% of cells (Fig. S3 I, black arrows). This flipping may result from the lack of PopZ-mediated anchoring of one of the *parS*–ParB complexes when the second one is segregated by ParA. Interestingly, flipping only ever occurred once before the final separation of the MipZ foci. Residual PopZ may be concentrated at one of the two cell poles; hence, if pairing occurred at a pole with very little PopZ, the paired complexes may flip before they can be resegregated. Collectively, our data support the idea that PopZ is not essential for chromosome resegregation after DSB repair but promotes the robustness of the process.

ParA is not essential for segregation of origin-distal regions after DSB repair

Our aforementioned results indicated that a DSB occurring ~200 kb from the origin translocated across the cell, paired with its homologous sister, and was then resegregated without disturbing the polar anchoring of the origin region (Fig. 4 B). To test whether this pattern holds for other, more distant chromosomal regions, we introduced an I-SceI site ~780 kb from the origin and visualized the cut site using the *parS*-YFP-ParB^{pMT1} system and the origin region using MipZ-CFP. 1 h after DSB induction, 96% of cells with one ParB^{pMT1} focus still had two MipZ foci, suggesting that induction of an origin-distal DSB resulted in pairing of the cut site but had no effect on the polar localization of MipZ-CFP (Fig. 6 A).

To test whether the left and right arms of the chromosome move together during DSB repair, we used the *parS*-mCherry-ParB^{P1} system to visualize a marker 3,042 kb from the origin, the equivalent position as the DSB site at ~780 kb but on the other chromosomal arm. Interestingly, although the left and right arms of the chromosome are positioned collinearly on the long axis of the cell (Le et al., 2013), they moved independently during homology search. 1 h after DSB induction, 94% of cells with one ParB^{pMT1} focus (marking a locus at ~800 kb) had two ParB^{P1} foci (marking a locus at 3,042 kb; Fig. 6 B).

Because polar anchoring of the origin region was largely unperturbed when a DSB occurred away from the origin, we wondered whether ParA was required for resegregation of origin-distal loci. We therefore simultaneously visualized ParA-YFP and the cut site introduced ~780 kb from the origin using the *parS*-CFP-ParB^{pMT1} system. Although we observed pairing and resegregation of the cut site, we did not typically observe substantial changes in the distribution of ParA-YFP (Fig. 6, C and D). When a DSB was introduced 30 kb from the origin, a ParA-YFP cloud

Downloaded from http://rupress.org/jcb/article-pdf/210/3/385/1591488/jcb_201505019.pdf by guest on 07 February 2026

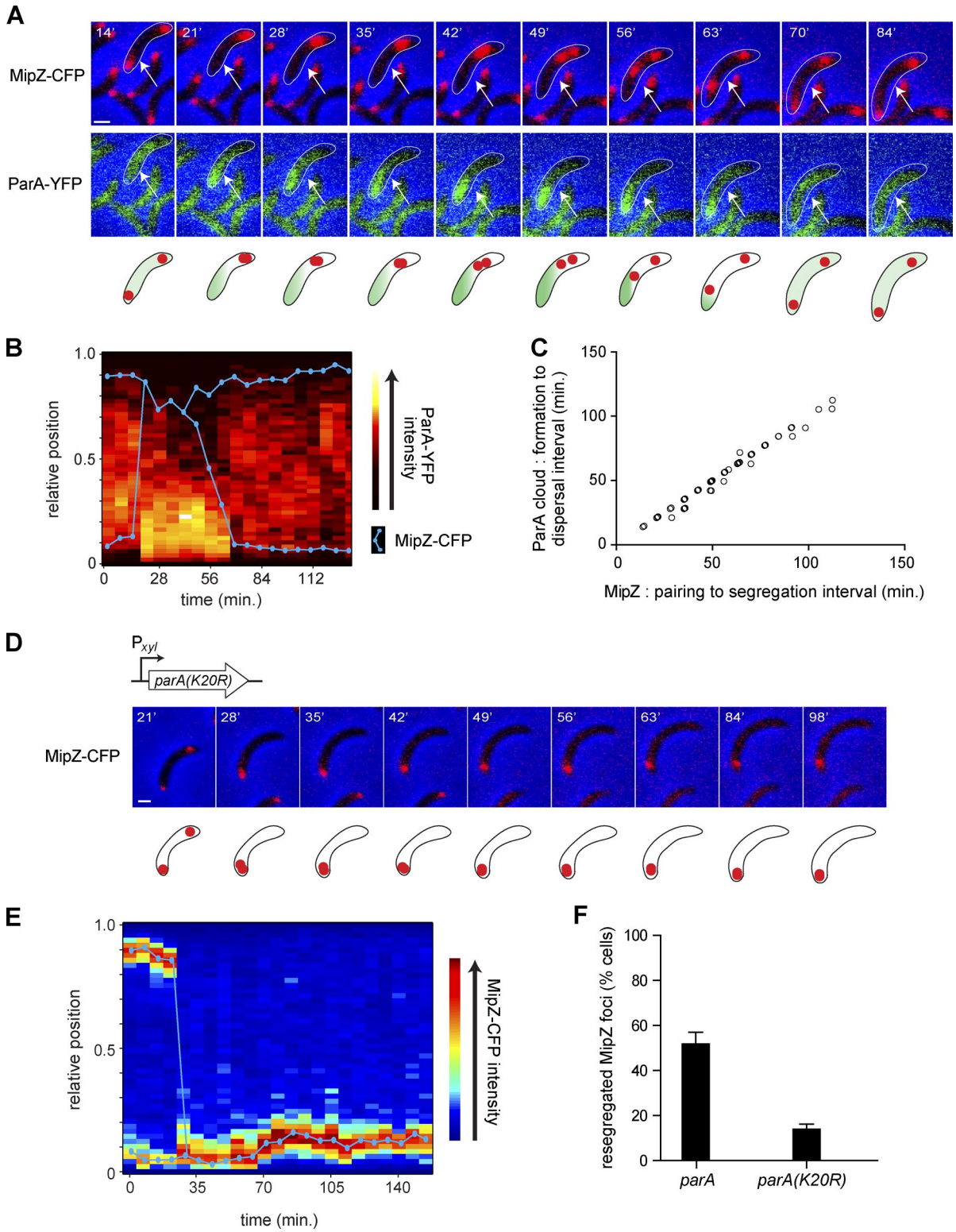

Figure 5. **ParA is essential for resegregation of the origin region after DSB repair.** (A) Representative time-lapse images showing dynamics of MipZ-CFP (red) and ParA-YFP (green) during DSB repair. Representative cells are highlighted with arrows. Schematic of cells shown below. (B) Kymograph of ParA-YFP dynamics in cell from A; MipZ-CFP trace in blue. (C) Scatterplot showing time between MipZ pairing and resegregation on the x axis and time between ParA cloud formation and dispersal on the y axis. n = 68 cells from a representative experiment out of two independent repeats. (D) Time-lapse microscopy showing that MipZ-CFP foci do not resegregate after pairing when *parA(K20R)-YFP*, a dominant-negative mutant, is expressed for 60 min before DSB induction. (E) Kymograph of MipZ-CFP dynamics for cell in D. (F) Summary of MipZ resegregation dynamics after a DSB and focus pairing in cells expressing either *parA-YFP* or *parA(K20R)-YFP* from the P_{xyl} promoter. Error bars represent SD, n = 110 cells from two independent repeats in each case. Bars, 1 µm.

Downloaded from http://rupress.org/jcb/article-pdf/210/3/385/1591488/jcb_201505019.pdf by guest on 07 February 2026

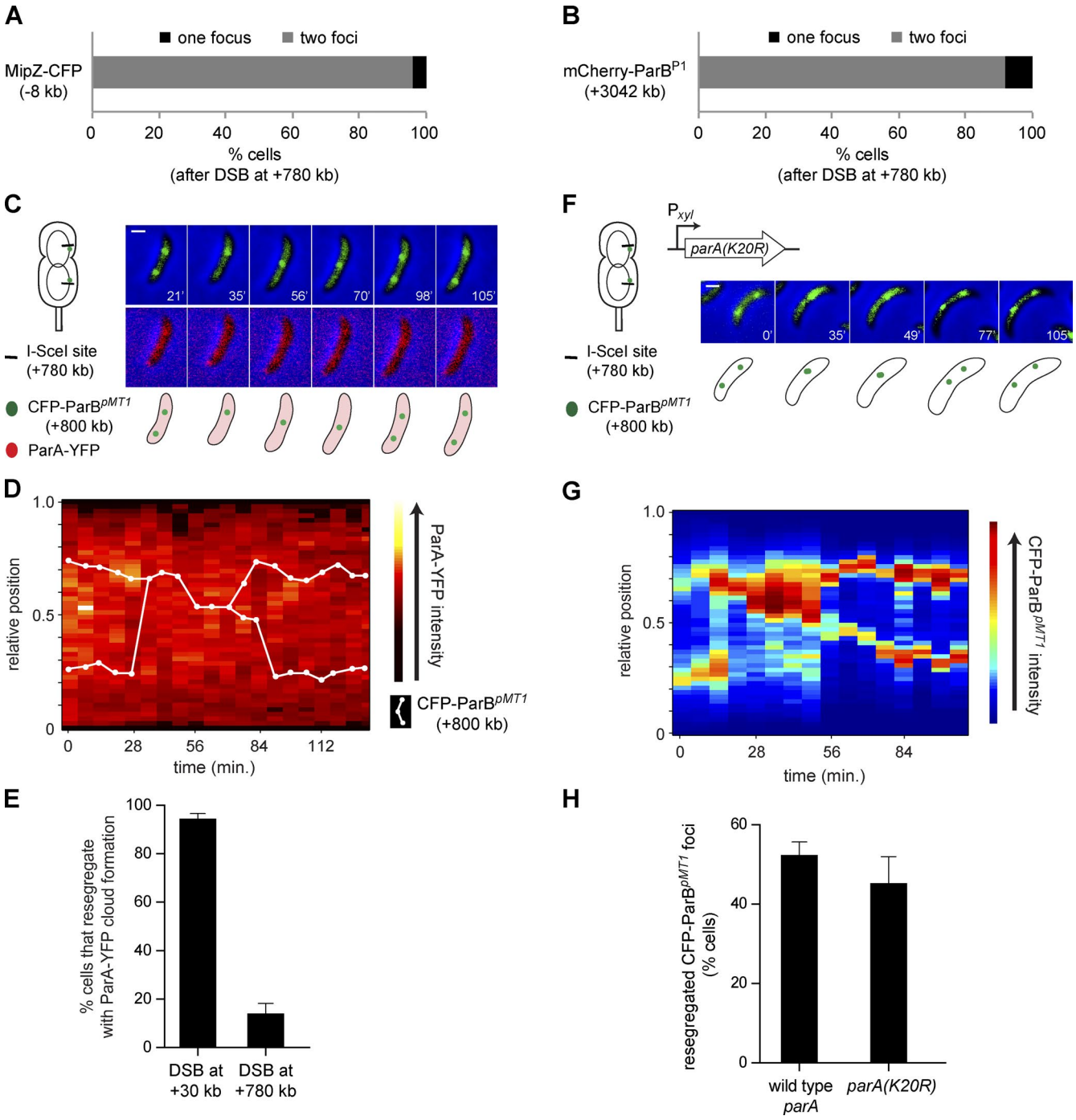

Figure 6. **ParA is not essential for resegregation of origin-distal regions after DSB repair.** (A) Summary of the number of MipZ-CFP foci in cells with one, paired focus of YFP-ParB^{pMT1}, which labels a site at 800 kb (the I-SceI induced DSB occurs at 780 kb from the origin). n = 150 from a representative experiment out of three independent repeats. (B) Summary of the number of mCherry-ParB^{P1} foci (which mark a site 3,042 kb from the origin) in those cells with one, paired YFP-ParB^{pMT1} focus (which marks a site at 800 kb); the I-SceI induced DSB occurs at 780 kb from the origin. n = 150 from a representative experiment out of three independent repeats. (C) Time-lapse microscopy showing pairing and resegregation of CFP-ParB^{pMT1} foci (green) 800 kb from the origin when a DSB occurs 780 kb from the origin. ParA-YFP shown in red. Images were taken every 7 min. (D) Kymograph of ParA-YFP dynamics from the cell shown in C. Pairing and resegregation of CFP-ParB^{pMT1} foci is overlaid as a trace (white line). (E) Summary of cells exhibiting ParA-YFP cloud formation coincident with resegregation after a DSB 30 kb or 780 kb from the origin. Error bars represent SD, n = 100 from two independent repeats in each case. (F) Time-lapse microscopy showing pairing and resegregation of CFP-ParB^{pMT1} foci 800 kb from the origin when a DSB is induced 780 kb from the origin, and the dominant-negative mutant *parA(K20R)-YFP* is expressed 60 min before imaging. (G) Kymograph of CFP-ParB^{pMT1} dynamics from cell shown in F. (H) Summary of the resegregation of CFP-ParB^{pMT1} foci labeling a site 800 kb from the origin after a DSB at 780 kb while expressing either wild-type *parA-YFP* or *parA(K20R)-YFP*. $n \geq 80$ in each case from two independent repeats. Error bars represent SD between imaging fields. Bars, 1 µm.

was observed in 95% of cells in which pairing and repair occurred. In contrast, upon introduction of a DSB 780 kb from the origin, only 14% of cells exhibiting a repair event displayed ParA-YFP cloud formation during resegregation (Fig. 6 E). Furthermore, resegregation remained largely unaffected when overexpressing the ParA(K20R) dominant-negative mutant (Fig. 6, E–G). Thus,

Downloaded from http://rupress.org/jcb/article-pdf/210/3/385/1591488/jcb_201505019.pdf by guest on 07 February 2026

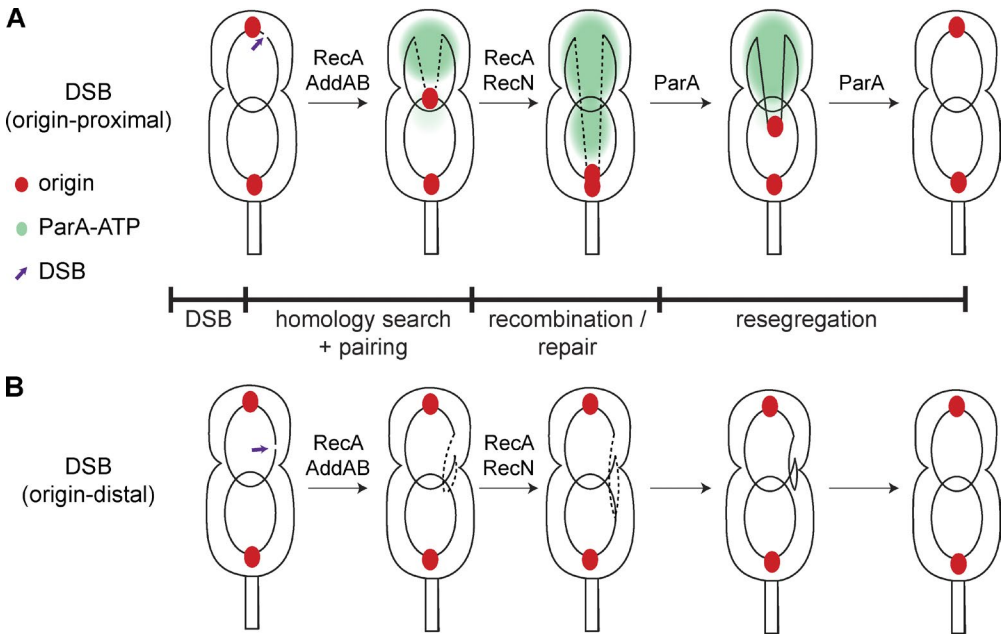

Figure 7. **The spatial dynamics of DSB repair in *C. crescentus*.** After a DSB occurs, the broken DNA region (purple arrow) is processed by the helicase-nuclease AddAB followed by ssDNA binding by RecA, which initiates the homology search process and pairing of a limited stretch of chromosomal DNA (dotted line). After repair via homologous recombination, the repaired DNA region is resegregated to its original position. The entire process can occur independent of ongoing DNA replication and without disrupting global chromosome organization. (A) For origin-proximal DSBs, resegregation requires ParA. Pairing of the origin region results in reformation of a ParA cloud, likely representing a pool of ATP-bound ParA. During resegregation, the ParA cloud retracts until the origin has been resegregated to the cell pole (similar to origin segregation dynamics after DNA replication). (B) For origin-distal DSBs, resegregation occurs in a ParA-independent manner, and the origin region remains anchored to the cell poles during the pairing and resegregation process. Similar to the stress–relaxation mechanism that drives chromosome segregation in *E. coli*, an elastic/spring-like force may resegregate sister chromosome loci after DSB repair without the need for a dedicated segregation machinery or ongoing replication. The overall structure and positioning of the chromosome, which is largely unperturbed by a DSB, may aid this process of resegregation.

we conclude that although ParA is essential for resegregating origin-proximal regions that suffer a DSB, other chromosomal regions can pair and resegregate independent of ParA.

Discussion

The dynamics of DSB repair in *C. crescentus*

The efficient repair of DSBs is essential for cell viability. Although DSB repair via homologous recombination has been well studied and key players in the repair process were identified, little is known about the spatial organization of this process inside cells and its relationship to DNA replication and chromosome segregation. Here, we showed that DSB repair can occur independently of ongoing DNA replication and whether the break occurs near or away from the origin of replication. A recent study in *E. coli* also showed that segregated chromosomal regions can engage in DSB repair (Lesterlin et al., 2014) but only examined cells in which DNA replication was ongoing. The fact that a DSB can be detected and repaired in the absence of DNA replication contrasts with other types of DNA damage that require passage of a replication fork past a lesion (Salles and Defais, 1984; Sassanfar and Roberts, 1990).

Our results support a model in which the chromosome that experiences a DSB becomes highly mobile, initiating a search for its homologous partner, which remains relatively stationary (Fig. 7). This model is consistent with recent studies in yeast in which chromosomal loci near a DSB showed increased mean-squared displacement in response to DSB induction (Dion et al., 2012; Miné-Hattab and Rothstein, 2012). Our fluorescent microscopy experiments indicate that only ~130 kb of DNA on either side of a DSB moves during the homologue pairing and recombination process. This number is comparable to a study in *E. coli*, in which chromosomal regions up to 80 kb from the cut site displayed colocalization with the cut site upon DSB induction (Shee et al., 2013). The global organization and domain structure of chromosomes is maintained during DSB repair. Additionally, our results indicate that homologous loci pair near where the undamaged locus resided, rather than at a dedicated "repair center," as previously suggested in *Bacillus subtilis* (Kidane and Graumann, 2005). Localizing repair to the site of the undamaged chromosome may help minimize other, unwanted disruptions to chromosome organization during repair and may help template the subsequent resegregation of paired loci (discussed in ParA-dependent and -independent chromosome resegregation).

DSB repair requires RecA but does not turn on the SOS response

The process of homologue pairing is dynamic in *C. crescentus* and occurred on a similar timescale as seen in *E. coli* (Lesterlin et al., 2014), usually within 5–7 min of the initial movement of one fluorescently tagged chromosomal locus. Although rapid, this initial movement sometimes involved back-and-forth movements in the x–y plane imaged. These results are consistent with the notion that a damaged chromosome searches the cell until pairing occurs rather than moving deterministically.

What drives the movement of chromosomal loci during homology search? Extensive work in bacteria has identified a

Downloaded from http://rupress.org/jcb/article-pdf/210/3/385/1591488/jcb_201505019.pdf by guest on 07 February 2026

set of conserved proteins that participate in the early steps of homology search and pairing (Dillingham and Kowalczykowski, 2008; Alonso et al., 2013). Several of these, including AddAB, RecN, and RecA, are required for the chromosomal dynamics documented here. AddAB is a helicase–nuclease complex involved in processing the DNA ends produced by a DSB; this processing likely prepares the DNA for movement, but AddAB is less likely to be involved in movement per se. Similarly, RecN, which is related to SMC proteins, may hold onto or somehow structure the damaged DNA in a manner important for movement but likely does not actively move damaged chromosomes. However, RecA may actively participate in the movement process. RecA binds ssDNA, such as that produced by AddAB during resection of the DNA ends produced by a DSB (Spies, 2013). In addition, RecA-GFP forms distinct foci or extended subcellular structures after DSB induction in *C. crescentus* and in *E. coli* and *B. subtilis* (Kidane and Graumann, 2005; Simmons et al., 2007; Lesterlin et al., 2014). The *E. coli* studies have further suggested that RecA bridges a broken chromosome and its intact homologous partner (Forget and Kowalczykowski, 2012; Lesterlin et al., 2014), possibly providing the force needed for a homology search and pairing to occur. However, the precise nature of the structures observed with fluorescently tagged RecA, which is not fully functional in *E. coli* or *C. crescentus*, remains unclear and should be a focus of future studies.

RecA is also required to induce the SOS system, as RecA bound to ssDNA stimulates autocleavage of LexA (Erill et al., 2007). Notably, however, the SOS response is not activated in most *C. crescentus* cells experiencing a single DSB. A similar finding was reported in *B. subtilis* (Simmons et al., 2009). Although the SOS response was reported to be activated in *E. coli* cells experiencing a single DSB (Pennington and Rosenberg, 2007), a recent study of *E. coli* showed that the large RecA-GFP filaments that formed in response to a DSB did not require new synthesis (Lesterlin et al., 2014). Collectively, these findings imply that (a) the RecA-YFP structures observed by epifluorescence microscopy after a DSB are assembled using existing pools of RecA and (b) the set of proteins needed for homology search, pairing, and DSB repair are either constitutively produced or induced in an SOS-independent manner. In *C. crescentus*, a DNA damage-induced, but SOS-independent system involving the transcription factor DriD was recently discovered. That initial study showed that DriD responds more strongly than LexA after treatment with zeocin, which induces DSBs (Modell et al., 2014). However, we did not observe a strong induction of a DriD reporter, P_{didA}-*yfp*, in cells experiencing an I-SceI–induced DSB.

ParA-dependent and -independent chromosome resegregation

After pairing and repair, chromosomal loci resegregate to their approximate original locations, moving in a more unidirectional manner compared with the initial search as judged by epifluorescence imaging of a single x–y plane. Although post-DSB repair resegregation has been observed before (Lesterlin et al., 2014), almost nothing is understood about how it occurs. We found that when a DSB occurs near the origin of replication, the ParABS system is essential for resegregation of the repaired loci. Although normally dispersed and presumably in the ATP-hydrolyzed state in predivisional cells (Schofield et al., 2010), a DSB induced the rapid appearance of a ParA-YFP cloud. This cloud of ParA, likely representing a pool of ParA bound to ATP and poised to drive segregation, formed at approximately the same time that origins paired, with the ParA concentrated at the pole opposite the site of pairing. These results suggest that ParA may intrinsically sense an imbalance in ParB concentration at the cell poles, localizing away from regions of the cell with a high concentration of ParB, which stimulates ParA ATPase activity. Such a "just-in-time" localization mechanism would nicely couple the pairing of origin-proximal DNA with establishment of the machinery needed for resegregation. Once a DSB has been repaired, we envision ParA driving the resegregation of one of the two origins, mostly as it does during the initial segregation process that occurs with DNA replication (Fig. 7 A).

Our results also suggest that ParABS-mediated origin segregation can occur multiple times in the same cell cycle and that ParA activity is primarily modulated by ParB localization. Multiple lines of evidence support these conclusions. First, ParA-ATP cloud formation after a DSB occurs concomitantly with ParB delocalization from the cell pole. Additionally, in cells where ParB delocalizes from both cell poles, ParA clouds also then formed at both cell poles. These ParA clouds then retracted in both directions, resulting in the resegregation of ParB and their associated origins to opposite cell poles. Second, ParA cloud formation is dependent on ParB delocalization from at least one cell pole. A DSB induced ~800 kb from the origin region does not affect ParB localization, and hence, ParA localization also remains largely unperturbed in such cells. Third, consistent with the idea that ParA activity is primarily regulated by ParB, we found that PopZ, a protein that anchors the ParB–*parS* complex to the cell poles and may modulate ParA activity, is not essential for resegregation. Furthermore, in filamentous Δ*popZ* cells with multiple segregated origins, origins that were localized away from the cell poles could pair and resegregate, supporting the idea that ParA localization and activity are dependent on ParB concentration, but independent of PopZ and the cell poles. However, in Δ*popZ* cells, the resegregating origins often exhibited more back-and-forth movements along the long axis of the cell. The delay and differences in movement could result from a lack of PopZ-based anchoring of ParB–*parS* or a defect in ParA activity in the absence of PopZ (Laloux and Jacobs-Wagner, 2013; Ptacin et al., 2014).

In contrast to origin-proximal regions, the segregation of origin-distal loci after DSB repair did not require ParA or produce changes in ParA-YFP localization. As noted in the previous paragraph, this finding is consistent with the notion that the ParA structure needed for origin segregation assembles in response to the movement of ParB away from one cell pole, which does not happen when a DSB occurs distal to the origin. How, then, do other chromosomal regions resegregate after homologous recombination? We propose that a repaired locus springs, or snaps, back to its original position, which is effectively determined by the structure and organization of the rest of the chromosome, most of which does not move or change after a site-specific DSB (Fig. 3). Such a process may be similar to the movement seen during chromosome segregation in *E. coli* (Fisher et al., 2013; Kleckner et al., 2014). During DNA replication in *E. coli*, recently duplicated sections of the chromosome remain transiently cohesed together; elimination of the cohesion, including resolution of precatenanes by topoisomerase IV, then allows the rapid movement of sister loci to opposite sides of the cell. This movement is likely not driven by a dedicated protein or protein complex but instead may represent a sort of stress relaxation mechanism (Joshi et

Downloaded from http://rupress.org/jcb/article-pdf/210/3/385/1591488/jcb_201505019.pdf by guest on 07 February 2026

al., 2011; Fisher et al., 2013; Kleckner et al., 2014). We envision a similar mechanism driving the resegregation of sister loci after DSB repair. While engaged in homologous recombination, sister chromosomal loci are effectively cohesed together. Once repair is completed, an elastic or spring-like force may help restore the previously damaged locus to its approximate original position (Fig. 7 B).

Final perspective

Although much is known about the process of homologous recombination, our study has provided important insights into the spatial organization of this process and, importantly, the interplay between DSB repair and chromosome organization and segregation. Our work demonstrates that chromosomes are not statically positioned within cells, but instead can exhibit dramatic, dynamic movements to promote repair and maintain genomic integrity. The system and tools generated here provide a foundation for further exploring the molecular mechanisms and regulation of DSB repair in bacteria. Given the highly conserved nature of homologous recombination and the universality of physical principles governing chromosomes, we anticipate that this work will shed light on DSB repair mechanisms throughout biology.

Materials and methods

Bacterial strains and growth conditions

All strains, plasmids, and primers used are listed in Table S1, S2, and S3. Chromosomal integrations and deletions were made using either a two-step recombination method with a *sacB* counter-selection marker (Skerker et al., 2005) or using vectors described in Thanbichler et al. (2007). Transductions were performed using ΦCR30 (Ely, 1991). Strain construction details are provided in Table S1 and S2. Cultures of *C. crescentus* were grown at 30°C in peptone yeast extract and supplemented with antibiotics, as necessary, at appropriate concentrations. *C. crescentus* synchronies were performed on mid-exponential phase cultures following procedures described previously (Jonas et al., 2011). For induction of P_{lac}-*dnaA*, IPTG was added to a final concentration of 0.5 mM. For induction of a DSB during time-lapse imaging, agarose pads were supplemented with 2 µM vanillate unless otherwise indicated. To block cell division, cephalexin was added to a final concentration of 36 µg/ml in a culture after synchronization and in agarose pads. To observe pairing dynamics (with imaging at 1- or 2-min time intervals), cells were pretreated with 2 µM vanillate for 15 min before start of imaging. For the induction of *parA-YFP* or *parA(K20R)-YFP*, nonreplicating predivisional cells were grown with 0.03% xylose for 60 min before imaging. *recA-YFP* was induced for 90 min before imaging with 0.03% xylose. Xylose was added to a final concentration of 0.3% to induce *YFP-parB*^{pMT1}, *mCherry-parB*^{P1}, or *CFP-parB*^{pMT1} for 3 h before imaging, whereas *sspB*$_{EC}$ was induced with 0.3% xylose for 6 h before imaging. Agarose pads were also supplemented with xylose at appropriate concentrations during time-lapse imaging. Cumate was added to a final concentration of 100 µM for induction of to induce *CFP-parB*^{pMT1} from the P_{cumate} promoter for 3 h before imaging.

Fluorescence microscopy

Fluorescence microscopy was performed on a microscope (Axio Observer Z1; Carl Zeiss) with a 100×/1.4 NA oil immersion objective, digital camera (Orca-II C10600; Hamamatsu Photonics), and an illumination system (LED-Colibri; Carl Zeiss). Temperature was maintained at 30°C with the Temp Module S1 and heating insert P S1 (Carl Zeiss). Focus was maintained automatically using the Definite Focus system (Carl Zeiss). Cells were grown on peptone yeast extract + 1.5% low-melting agarose pads with xylose, vanillate, and cephalexin, as indicated, and imaged in a glass-bottomed Petri dish. Images were acquired every 1, 2, 5, or 7 min using the software MetaMorph (Universal Imaging). Image analysis was performed using MicrobeTracker (Sliusarenko et al., 2011) executed in Matlab or using ImageJ (National Institutes of Health). Fluorescent spots were detected using the Spotfinder function in Microbetracker or counted using the cell counter function in ImageJ. Kymographs were also generated using the kymograph function in MicrobeTracker. Image overlays were generated using ImageJ. In cells with more than one pairing event, only the first event was counted. For cells with only a single MipZ or ParB^{pMT1} focus in Fig. 3, we analyzed only those cells in which the intensity of the single MipZ focus was at least 1.6 times that of cells harboring two foci (presumably as a result of pairing of the DNA regions during repair). ParA cloud formation was defined as loss of homogenous distribution of YFP intensity across the cell area and concentration of YFP intensity toward a cell pole. For Fig. 5 F and Fig. 6 H, resegregation of paired foci was defined as the ability observe two discernable fluorescent foci that were ≥1 µm apart. Scale bars in figures are 1 µm.

Hi-C

For Hi-C experiments, *C. crescentus* cells were depleted of DnaA for 1.5 h before synchronization. Swarmer cells were then released into DnaA-depleting conditions (without IPTG), and DSBs were induced for 1 h by the addition of 500 µM vanillate. Formaldehyde (Sigma-Aldrich) was then added to a final concentration of 1%. Formaldehyde cross-links protein–DNA and DNA–DNA together, thereby capturing the structure of the chromosome at the time of fixation. Fixation was performed with cells at an OD_{600} of 0.2. The cross-linking reactions were allowed to proceed for 30 min at 25°C before quenching with glycine at a final concentration of 0.125 M. Fixed cells were then pelleted by centrifugation and subsequently washed twice with M2 buffer (6.1 mM Na_2HPO_4, 3.9 mM KH_2PO_4, 9.3 mM NH_4Cl, 0.5 mM $MgSO_4$, 10 µM $FeSO_4$, and 0.5 mM $CaCl_2$) before resuspending in TE buffer (10 mM Tris-HCl, pH 8.0, and 1 mM EDTA) to a final concentration of 10^7 cells/µl. Resuspended cells were then divided into 25-µl aliquots and stored at −80°C for no more than 2 wk. Each Hi-C experiment was performed using two of the 25-µl aliquots. Chromosome conformation capture with next-generation sequencing (Hi-C) was performed exactly as described in Le et al. (2013). To each 25-µl aliquot, 2,000 U Ready-Lyse Lysozyme (Epicenter) was added and incubated for 15 min before addition of SDS to a final concentration of 0.25% for an additional 15 min to completely dissolve cell membranes and to release chromosomal DNA. The DNA was then digested with BglII restriction enzyme in a total reaction of 50 µl. The DNA was digested to completion by incubating at 37°C for 3 h. The reaction was cooled on ice before labeling overhangs with biotin-labeled deoxy-ATP (Invitrogen). Labeling was performed at 25°C for 45 min before addition of SDS to a final concentration of 0.5% to stop the reaction. Blunted DNA ends were then ligated together in very dilute conditions so that DNA fragments that were spatially close in vivo and fixed together by formaldehyde treatment would be ligated while minimizing ligation between randomly colliding DNA fragments. The ligation reaction was incubated at 16°C for 4 h. After ligation, EDTA was added to a final concentration of 10 mM to stop the reaction, and 2.5 µl of 20 mg/ml Proteinase K (New England Biolabs, Inc.) was added. The reaction was then incubated at 65°C overnight to reverse cross-links. DNA was subsequently extracted twice by phenol/chloroform/isoamyl alcohol, precipitated by isopropanol. Nonligated, but biotin-labeled, fragments were eliminated using the 3′–5′ exonuclease activity of T4 polymerase. DNA was then extracted using phenol/chloroform/isoamyl alcohol

Downloaded from http://rupress.org/jcb/article-pdf/210/3/385/1591488/jcb_201505019.pdf by guest on 07 February 2026

and precipitated using isopropanol. Purified DNA was then sheared to between 200 and 600 bp using the Bioruptor (Diagnogen). DNA was then end repaired. Repaired DNA then had 3′-A overhangs created by Klenow 3′–5′ exo⁻ (New England Biolabs, Inc.). This DNA was then ligated with standard Y-shaped Illumina adaptors. In the next step, biotin-labeled junctions were purified from nonlabeled junctions using Streptavidin Dynabeads (Invitrogen). Washed beads were introduced into the ligation mixture above and incubated with gentle agitation for 30 min to capture biotin-labeled DNA junctions. Beads were then pulled down magnetically, and unwanted supernatant was discarded. Beads with biotin-labeled DNA fragments bound were then washed twice and then resuspended in 10 µl of water. DNA bound to beads was then enriched by PCR using primers compatible with paired-end sequencing (Illumina). PCR products were then purified by gel extraction before sequencing on an Illumina HiSeq 2000 (Massachusetts Institute of Technology BioMicroCenter). Because Hi-C was performed on G1-phase swarmer cells in which DSBs are not repaired and break ends are resected and eventually degraded, we only used Hi-C data to infer the global chromosome conformation, not the local chromosomal state at the break site; the ssDNA near the cut site will not behave like double-stranded DNA during the Hi-C procedure. Hi-C data were deposited in GEO (GSE66811).

Western blotting

Cells were pelleted and then resuspended in SDS sample buffer and heated to 95°C for 5 min. Equal amounts of total protein were run on 10% Tris-HCl gels (Bio-Rad Laboratories, Inc.) at 150 V for separation. Resolved proteins were transferred to polyvinylidene fluoride membranes and probed with 1:5,000 dilution of primary antibodies against PopZ (G. Bowman, University of Wyoming, Laramie, WY; Bowman et al., 2008) or RpoA (Sigma-Aldrich) and secondary horseradish peroxidase–conjugated antibody (1:5,000). Blots were visualized using a FluorChem M imager (ProteinSimple).

Semiquantitative PCR

C. crescentus cells were grown to OD_{600} of ~0.1, and the DSB was induced (cut) by addition of 10 µM vanillate for 1 h. Control cells were grown in the absence of vanillate (no cut), 1 ml of cells were pelleted, and genomic DNA was isolated. Semi-quantitative PCR was performed for 15 cycles using Phusion polymerase across the cut site or at a control locus near the terminus region. Products were run on an agarose gel, and DNA was stained with ethidium bromide. Bands were quantified using ImageJ.

Online supplemental material

Fig. S1 provides data on the characterization of the I-SceI system in *C. crescentus*. Fig. S2 provides data summarizing DSB repair in replicating cells and on the essentiality of DSB repair proteins involved in homologous recombination. Fig. S2 also provides supporting evidence for origin resegregation after DSB repair in predivisional cells, ParB-MipZ colocalization, RecA filament formation, and ParA-YFP cloud formation. Fig. S3 shows data on the characterization of the role of PopZ in origin resegregation during DSB repair. Tables S1, S2, and S3 lists the strains, plasmids, and primers, respectively. Online supplemental material is available at http://www.jcb.org/cgi/content/full/jcb.201505019/DC1.

Acknowledgments

We thank X. Wang and K. Jonas for comments on the manuscript. We are grateful to D. Leach, C. Jacobs-Wagner, F. Boccard, and G. Bowman for reagents.

This work was supported by National Institutes of Health grant R01GM082899 (M.T. Laub), a Gordon and Betty Moore Foundation postdoctoral fellow of the Life Sciences Research Foundation (T.B.K. Le), and a Human Frontiers Science Program Postdoctoral Fellowship (A. Badrinarayanan). M.T. Laub is an Early Career Scientist of the Howard Hughes Medical Institute.

The authors declare no competing financial interests.

Submitted: 5 May 2015
Accepted: 16 June 2015

References

Alonso, J.C., P.P. Cardenas, H. Sanchez, J. Hejna, Y. Suzuki, and K. Takeyasu. 2013. Early steps of double-strand break repair in *Bacillus subtilis*. *DNA Repair (Amst.).* 12:162–176. http://dx.doi.org/10.1016/j.dnarep.2012.12.005

Bowman, G.R., L.R. Comolli, J. Zhu, M. Eckart, M. Koenig, K.H. Downing, W.E. Moerner, T. Earnest, and L. Shapiro. 2008. A polymeric protein anchors the chromosomal origin/ParB complex at a bacterial cell pole. *Cell.* 134:945–955. http://dx.doi.org/10.1016/j.cell.2008.07.015

Chen, Y.E., C. Tropini, K. Jonas, C.G. Tsokos, K.C. Huang, and M.T. Laub. 2011. Spatial gradient of protein phosphorylation underlies replicative asymmetry in a bacterium. *Proc. Natl. Acad. Sci. USA.* 108:1052–1057. http://dx.doi.org/10.1073/pnas.1015397108

Cromie, G.A., J.C. Connelly, and D.R.F. Leach. 2001. Recombination at double-strand breaks and DNA ends: conserved mechanisms from phage to humans. *Mol. Cell.* 8:1163–1174. http://dx.doi.org/10.1016/S1097-2765(01)00419-1

Dillingham, M.S., and S.C. Kowalczykowski. 2008. RecBCD enzyme and the repair of double-stranded DNA breaks. *Microbiol. Mol. Biol. Rev.* 72:642–671. http://dx.doi.org/10.1128/MMBR.00020-08

Dion, V., V. Kalck, C. Horigome, B.D. Towbin, and S.M. Gasser. 2012. Increased mobility of double-strand breaks requires Mec1, Rad9 and the homologous recombination machinery. *Nat. Cell Biol.* 14:502–509. http://dx.doi.org/10.1038/ncb2465

Ebersbach, G., A. Briegel, G.J. Jensen, and C. Jacobs-Wagner. 2008. A self-associating protein critical for chromosome attachment, division, and polar organization in *caulobacter*. *Cell.* 134:956–968. http://dx.doi.org/10.1016/j.cell.2008.07.016

Ely, B. 1991. Genetics of *Caulobacter crescentus*. *Methods Enzymol.* 204:372–384. http://dx.doi.org/10.1016/0076-6879(91)04019-K

Erill, I., S. Campoy, and J. Barbé. 2007. Aeons of distress: an evolutionary perspective on the bacterial SOS response. *FEMS Microbiol. Rev.* 31:637–656. http://dx.doi.org/10.1111/j.1574-6976.2007.00082.x

Fisher, J.K., A. Bourniquel, G. Witz, B. Weiner, M. Prentiss, and N. Kleckner. 2013. Four-dimensional imaging of *E. coli* nucleoid organization and dynamics in living cells. *Cell.* 153:882–895. http://dx.doi.org/10.1016/j.cell.2013.04.006

Forget, A.L., and S.C. Kowalczykowski. 2012. Single-molecule imaging of DNA pairing by RecA reveals a three-dimensional homology search. *Nature.* 482:423–427. http://dx.doi.org/10.1038/nature10782

Huitema, E., S. Pritchard, D. Matteson, S.K. Radhakrishnan, and P.H. Viollier. 2006. Bacterial birth scar proteins mark future flagellum assembly site. *Cell.* 124:1025–1037. http://dx.doi.org/10.1016/j.cell.2006.01.019

Jonas, K., Y.E. Chen, and M.T. Laub. 2011. Modularity of the bacterial cell cycle enables independent spatial and temporal control of DNA replication. *Curr. Biol.* 21:1092–1101. http://dx.doi.org/10.1016/j.cub.2011.05.040

Joshi, M.C., A. Bourniquel, J. Fisher, B.T. Ho, D. Magnan, N. Kleckner, and D. Bates. 2011. *Escherichia coli* sister chromosome separation includes an abrupt global transition with concomitant release of late-splitting intersister snaps. *Proc. Natl. Acad. Sci. USA.* 108:2765–2770. http://dx.doi.org/10.1073/pnas.1019593108

Kidane, D., and P.L. Graumann. 2005. Dynamic formation of RecA filaments at DNA double strand break repair centers in live cells. *J. Cell Biol.* 170:357–366. http://dx.doi.org/10.1083/jcb.200412090

Kiekebusch, D., K.A. Michie, L.-O. Essen, J. Löwe, and M. Thanbichler. 2012. Localized dimerization and nucleoid binding drive gradient formation by the bacterial cell division inhibitor MipZ. *Mol. Cell.* 46:245–259. http://dx.doi.org/10.1016/j.molcel.2012.03.004

Downloaded from http://rupress.org/jcb/article-pdf/210/3/385/1591488/jcb_201505019.pdf by guest on 07 February 2026

Kleckner, N., J.K. Fisher, M. Stouf, M.A. White, D. Bates, and G. Witz. 2014. The bacterial nucleoid: nature, dynamics and sister segregation. *Curr. Opin. Microbiol.* 22:127–137. http://dx.doi.org/10.1016/j.mib.2014.10.001

Krajewski, W.W., X. Fu, M. Wilkinson, N.B. Cronin, M.S. Dillingham, and D.B. Wigley. 2014. Structural basis for translocation by AddAB helicase-nuclease and its arrest at χ sites. *Nature.* 508:416–419. http://dx.doi.org/10.1038/nature13037

Laloux, G., and C. Jacobs-Wagner. 2013. Spatiotemporal control of PopZ localization through cell cycle–coupled multimerization. *J. Cell Biol.* 201:827–841. http://dx.doi.org/10.1083/jcb.201303036

Lam, H., W.B. Schofield, and C. Jacobs-Wagner. 2006. A landmark protein essential for establishing and perpetuating the polarity of a bacterial cell. *Cell.* 124:1011–1023. http://dx.doi.org/10.1016/j.cell.2005.12.040

Le, T.B., and M.T. Laub. 2014. New approaches to understanding the spatial organization of bacterial genomes. *Curr. Opin. Microbiol.* 22:15–21. http://dx.doi.org/10.1016/j.mib.2014.09.014

Le, T.B.K., M.V. Imakaev, L.A. Mirny, and M.T. Laub. 2013. High-resolution mapping of the spatial organization of a bacterial chromosome. *Science.* 342:731–734. http://dx.doi.org/10.1126/science.1242059

Lenhart, J.S., J.W. Schroeder, B.W. Walsh, and L.A. Simmons. 2012. DNA repair and genome maintenance in *Bacillus subtilis. Microbiol. Mol. Biol. Rev.* 76:530–564. http://dx.doi.org/10.1128/MMBR.05020-11

Lesterlin, C., G. Ball, L. Schermelleh, and D.J. Sherratt. 2014. RecA bundles mediate homology pairing between distant sisters during DNA break repair. *Nature.* 506:249–253. http://dx.doi.org/10.1038/nature12868

Lim, H.C., I.V. Surovtsev, B.G. Beltran, F. Huang, J. Bewersdorf, and C. Jacobs-Wagner. 2014. Evidence for a DNA-relay mechanism in ParABS-mediated chromosome segregation. *eLife.* 3:e02758. http://dx.doi.org/10.7554/eLife.02758

Livny, J., Y. Yamaichi, and M.K. Waldor. 2007. Distribution of centromere-like *parS* sites in bacteria: insights from comparative genomics. *J. Bacteriol.* 189:8693–8703. http://dx.doi.org/10.1128/JB.01239-07

Miné-Hattab, J., and R. Rothstein. 2012. Increased chromosome mobility facilitates homology search during recombination. *Nat. Cell Biol.* 14:510–517. http://dx.doi.org/10.1038/ncb2472

Modell, J.W., A.C. Hopkins, and M.T. Laub. 2011. A DNA damage checkpoint in *Caulobacter crescentus* inhibits cell division through a direct interaction with FtsW. *Genes Dev.* 25:1328–1343. http://dx.doi.org/10.1101/gad.2038911

Modell, J.W., T.K. Kambara, B.S. Perchuk, and M.T. Laub. 2014. A DNA damage-induced, SOS-independent checkpoint regulates cell division in *Caulobacter crescentus. PLoS Biol.* 12:e1001977. http://dx.doi.org/10.1371/journal.pbio.1001977

Mohl, D.A., J. Easter Jr., and J.W. Gober. 2001. The chromosome partitioning protein, ParB, is required for cytokinesis in *Caulobacter crescentus. Mol. Microbiol.* 42:741–755. http://dx.doi.org/10.1046/j.1365-2958.2001.02643.x

Monteilhet, C., A. Perrin, A. Thierry, L. Colleaux, and B. Dujon. 1990. Purification and characterization of the in vitro activity of I-Sce I, a novel and highly specific endonuclease encoded by a group I intron. *Nucleic Acids Res.* 18:1407–1413. http://dx.doi.org/10.1093/nar/18.6.1407

Nielsen, H.J., Y. Li, B. Youngren, F.G. Hansen, and S. Austin. 2006. Progressive segregation of the *Escherichia coli* chromosome. *Mol. Microbiol.* 61:383–393. http://dx.doi.org/10.1111/j.1365-2958.2006.05245.x

Pellegrino, S., J. Radzimanowski, D. de Sanctis, E. Boeri Erba, S. McSweeney, and J. Timmins. 2012. Structural and functional characterization of an SMC-like protein RecN: new insights into double-strand break repair. *Structure.* 20:2076–2089. http://dx.doi.org/10.1016/j.str.2012.09.010

Pennington, J.M., and S.M. Rosenberg. 2007. Spontaneous DNA breakage in single living *Escherichia coli* cells. *Nat. Genet.* 39:797–802. http://dx.doi.org/10.1038/ng2051

Ptacin, J.L., S.F. Lee, E.C. Garner, E. Toro, M. Eckart, L.R. Comolli, W.E. Moerner, and L. Shapiro. 2010. A spindle-like apparatus guides bacterial chromosome segregation. *Nat. Cell Biol.* 12:791–798. http://dx.doi.org/10.1038/ncb2083

Ptacin, J.L., A. Gahlmann, G.R. Bowman, A.M. Perez, A.R.S. von Diezmann, M.R. Eckart, W.E. Moerner, and L. Shapiro. 2014. Bacterial scaffold directs pole-specific centromere segregation. *Proc. Natl. Acad. Sci. USA.* 111:E2046–E2055. http://dx.doi.org/10.1073/pnas.1405188111

Rood, K.L., N.E. Clark, P.R. Stoddard, S.C. Garman, and P. Chien. 2012. Adaptor-dependent degradation of a cell-cycle regulator uses a unique substrate architecture. *Structure.* 20:1223–1232. http://dx.doi.org/10.1016/j.str.2012.04.019

Salles, B., and M. Defais. 1984. Signal of induction of recA protein in *E. coli. Mutat. Res.* 131:53–59.

Sassanfar, M., and J.W. Roberts. 1990. Nature of the SOS-inducing signal in *Escherichia coli*. The involvement of DNA replication. *J. Mol. Biol.* 212:79–96. http://dx.doi.org/10.1016/0022-2836(90)90306-7

Schofield, W.B., H.C. Lim, and C. Jacobs-Wagner. 2010. Cell cycle coordination and regulation of bacterial chromosome segregation dynamics by polarly localized proteins. *EMBO J.* 29:3068–3081. http://dx.doi.org/10.1038/emboj.2010.207

Shebelut, C.W., J.M. Guberman, S. van Teeffelen, A.A. Yakhnina, and Z. Gitai. 2010. *Caulobacter* chromosome segregation is an ordered multistep process. *Proc. Natl. Acad. Sci. USA.* 107:14194–14198. http://dx.doi.org/10.1073/pnas.1005274107

Shee, C., B.D. Cox, F. Gu, E.M. Luengas, M.C. Joshi, L.-Y. Chiu, D. Magnan, J.A. Halliday, R.L. Frisch, J.L. Gibson, et al. 2013. Engineered proteins detect spontaneous DNA breakage in human and bacterial cells. *eLife.* 2:e01222. http://dx.doi.org/10.7554/eLife.01222

Simmons, L.A., A.D. Grossman, and G.C. Walker. 2007. Replication is required for the RecA localization response to DNA damage in *Bacillus subtilis. Proc. Natl. Acad. Sci. USA.* 104:1360–1365. http://dx.doi.org/10.1073/pnas.0607123104

Simmons, L.A., A.I. Goranov, H. Kobayashi, B.W. Davies, D.S. Yuan, A.D. Grossman, and G.C. Walker. 2009. Comparison of responses to double-strand breaks between *Escherichia coli* and *Bacillus subtilis* reveals different requirements for SOS induction. *J. Bacteriol.* 191:1152–1161. http://dx.doi.org/10.1128/JB.01292-08

Skerker, J.M., M.S. Prasol, B.S. Perchuk, E.G. Biondi, and M.T. Laub. 2005. Two-component signal transduction pathways regulating growth and cell cycle progression in a bacterium: a system-level analysis. *PLoS Biol.* 3:e334. http://dx.doi.org/10.1371/journal.pbio.0030334

Sliusarenko, O., J. Heinritz, T. Emonet, and C. Jacobs-Wagner. 2011. High-throughput, subpixel precision analysis of bacterial morphogenesis and intracellular spatio-temporal dynamics. *Mol. Microbiol.* 80:612–627. http://dx.doi.org/10.1111/j.1365-2958.2011.07579.x

Spies, M. 2013. There and back again: new single-molecule insights in the motion of DNA repair proteins. *Curr. Opin. Struct. Biol.* 23:154–160. http://dx.doi.org/10.1016/j.sbi.2012.11.008

Symington, L.S., and J. Gautier. 2011. Double-strand break end resection and repair pathway choice. *Annu. Rev. Genet.* 45:247–271. http://dx.doi.org/10.1146/annurev-genet-110410-132435

Thanbichler, M., and L. Shapiro. 2006. MipZ, a spatial regulator coordinating chromosome segregation with cell division in *Caulobacter. Cell.* 126:147–162. http://dx.doi.org/10.1016/j.cell.2006.05.038

Thanbichler, M., A.A. Iniesta, and L. Shapiro. 2007. A comprehensive set of plasmids for vanillate- and xylose-inducible gene expression in *Caulobacter crescentus. Nucleic Acids Res.* 35:e137. http://dx.doi.org/10.1093/nar/gkm818

Toro, E., S.-H. Hong, H.H. McAdams, and L. Shapiro. 2008. *Caulobacter* requires a dedicated mechanism to initiate chromosome segregation. *Proc. Natl. Acad. Sci. USA.* 105:15435–15440. http://dx.doi.org/10.1073/pnas.0807448105

Viollier, P.H., M. Thanbichler, P.T. McGrath, L. West, M. Meewan, H.H. McAdams, and L. Shapiro. 2004. Rapid and sequential movement of individual chromosomal loci to specific subcellular locations during bacterial DNA replication. *Proc. Natl. Acad. Sci. USA.* 101:9257–9262. http://dx.doi.org/10.1073/pnas.0402606101

Wang, X., P. Montero Llopis, and D.Z. Rudner. 2013. Organization and segregation of bacterial chromosomes. *Nat. Rev. Genet.* 14:191–203. http://dx.doi.org/10.1038/nrg3375

Wigley, D.B. 2013. Bacterial DNA repair: recent insights into the mechanism of RecBCD, AddAB and AdnAB. *Nat. Rev. Microbiol.* 11:9–13. http://dx.doi.org/10.1038/nrmicro2917

Downloaded from http://rupress.org/jcb/article-pdf/210/3/385/1591488/jcb_201505019.pdf by guest on 07 February 2026